Int. J. Therm. Sci. (2000) 39, 514–518

S1290-0729(00)00230-1/FLA

Micron scale photothermal imaging [1]

Danièle Fournier, Benoît C. Forget *, Christine Boué, Jean Paul Roger

Équipe d'Instrumentation de l'UPMC, UPR A0005 du CNRS, ESPCI, 10 rue Vauquelin, 75005 Paris, France

(Received 1 October 1999, accepted 5 November 1999)

Abstract — In this paper, we present various experimental results which demonstrate the ability of photothermal methods to perform heat diffusion imaging at the micron scale. Photoreflectance microscopy measurements have been performed on a composite sample presenting a strong anisotropy of thermal properties and on microelectronic devices. We will then introduce the CCD array photothermal microscopy which permits the acquisition of a complete image in a single shot, without moving the sample. A stroboscopic technique must be used in order to adjust to the relatively low frame rate of the CCD camera. We will discuss two cases: homodyne and heterodyne detection. © 2000 Éditions scientifiques et médicales Elsevier SAS

photothermal imaging / microscale / composite materials / thermal anisotropy / microelectronic devices / CCD camera

Résumé — **Imagerie photothermique à l'échelle du micron.** Nous présentons dans cet article divers résultats expérimentaux qui démontrent la possibilité de réaliser par des méthodes photothermiques une imagerie de la diffusion de la chaleur à l'échelle du micron. Des mesures de microscopie photothermique ont été réalisées sur un échantillon composite présentant une forte anisotropie de ses propriétés thermiques et sur des composants de microélectronique. Nous introduirons ensuite le microscope à matrice de photodétecteurs qui permet l'acquisition en parallèle d'une image, sans avoir à déplacer l'échantillon. Une technique stroboscopique doit être employée pour pallier à la trop faible vitesse d'acquisition d'une caméra CCD. Nous présentons deux approches : la détection homodyne et la détection hétérodyne. © 2000 Éditions scientifiques et médicales Elsevier SAS

imagerie photothermique / microéchelle / materiaux composites / anisotropie thermique / composants microélectroniques / camera CCD

Nomenclature

f	modulation frequency
R, R_0, R_m	reflection coefficient, average (or DC) and modulated part
$\Phi, \Phi_0, \Phi_\mathrm{m}$	incident flux, average (or DC) and modulated part
φ	relative phase of the incident flux

0. INTRODUCTION

The aim of this paper is to demonstrate the ability of photothermal methods to image heat diffusion processes at micron scale. These methods measure the local temperature rise through its effect on the reflexion coefficient. The heat source is either an intensity modulated laser beam which heats the sample by conversion of the luminous energy to thermal energy, or the sample itself when biased electronic or optoelectronic circuits are investigated. These photothermal images at micron scale are interesting tools to determine the local diffusivity at single grain scale, to reveal thermal barriers at the grain boundaries and to look at heat diffusion in microelectronics circuits.

1. MONODETECTOR PHOTOTHERMAL MICROSCOPE

In order to obtain a thermal image with a micron scale, one possibility is to use visible light and to work with diffraction limited system. The sample is illuminated with a focused excitation spot (argon laser) and the probe beam is reflected at the surface of the sample, in the heated area. In order to obtain easily heated spots as small as a micrometer, we use a commercial microscope to fo-

* Correspondence and reprints.
forget@optique.espci.fr

[1] Based on a paper presented as a plenary talk at Eurotherm Seminar No. 57 "Microscale Heat Transfer", Poitiers, France, July 8–10, 1998.

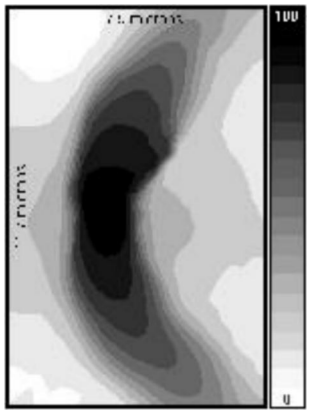

Figure 1. Monodetector photothermal image: 1 MHz phase photoreflectance signal on a carbon–carbon composite (from S. Hirschi CEA/SEP sample).

cus the heating beam. The probe beam is produced by a 670 nm diode laser. After reflection on the area of modulated heating, the probe beam is received on a silicon photodiode coupled with a high frequency lock-in amplifier. The lock-in amplifier permits extracting the thermally induced variation of the reflection coefficient, R_m, which is modulated at the same frequency as the argon laser or heat source. From the "DC" part the average reflection coefficient R_0 can be extracted. Furthermore, lock-in detection permits excellent signal-to-noise ratio: it is possible to achieve a sensitivity of 10^{-6} in R_m/R_0 with a frequency range spreading up to 20 MHz [1–3]. This experiment requires high modulation frequencies in order to prevent heat from diffusing on a large area.

We have done local thermal diffusivity measurements at the grain scale in various samples by varying the distance between the two beams and complete the study by the thermal barrier detection associated with the grain boundaries when the two beams are superimposed [4, 5]. *Figure 1* is a "phase" image of the photoreflectance signal recorded at 1 MHz on a carbon–carbon composite. The investigated area is 11.7×7.5 μm^2. This image shows clearly the strong anisotropy of the heat diffusion in this sample.

1.1. Imaging of devices

Heating in semiconductor devices is an important concern. We have achieved photothermal images of emitting laser diodes [6] and of biased MOSFET [7]. In this case we have superimposed to the bias current an alternative current in order to create a modulated heat field which was imaged with the probe beam. *Figure 2* is an example of such an image on a DFB laser diode. In order to get a full image we had to scan all the heated area. The time to obtain a full image is around one hour or more; such an acquisition time is a severe drawback of our method.

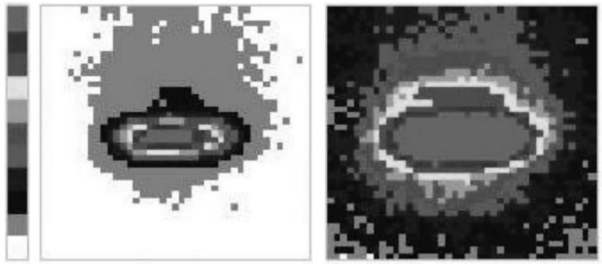

Figure 2. Amplitude (left) and phase (rigth) of the photoreflectance signal from a DFB laser diode. This image permits localization of the thermal source and detection of early sign of eventual failure.

2. CCD ARRAY PHOTOTHERMAL MICROSCOPE

In order to obtain the amplitude and phase of a modulated signal, in our case R_m the amplitude of the reflection coefficient variation and φ its phase, one can simply sample the signal and afterwards perform a Fourier transform. This idea has already been successfully employed in the field of infrared imaging [8, 9], where the modulated infrared emission is sampled.

We will now discuss how we have transposed this idea to photothermal imaging with two important improvements. The first has already been mentioned: it is the use of visible light which allows spatial resolution of less than 1 μm (as long as diffusion does not spread the heat away from the sources by more than roughly this distance), compared to the 5–10 μm achieved with infrared radiation.

We have replaced the photodiode by a matrix of 256×256 detectors with the goal of obtaining a full image in a few minutes. We use an analog Dalsa-CA-D1 camera limited to a 200 frames per second; which brings us to our second improvement. In order to correctly sample the signal we need to respect Shanon's sampling theorem which limits the modulation frequency of the heat source to one half of the camera maximal frame rate (often one quarter is used in order to simplify the amplitude and phase calculation). We have overcome this second problem by using a stroboscopic technique: the reflection coefficient and the incident probe are both modulated, this permits a mixing which shifts the thermal information towards low frequencies, thus

permitting sampling by the CCD camera. Depending on the modulation frequency of the probe two types of detection can be envisaged: homodyne or heterodyne.

2.1. Homodyne detection

The setup remains basically the same as described in Section 1, with two important differences: first, the single detector is obviously replaced by a CCD camera, and second, the probe laser is replaced by a LED and is itself modulated in intensity. In this first setup, the LED is modulated at the same frequency as the thermal source (see *figure 3*, left). The light reflected back to the CCD is expressed as the product of the reflection coefficient, R, by the incident flux, Φ:

$$\begin{aligned}\Phi \cdot R = &\left(\Phi_0 + \Phi_\mathrm{m}\cos(2\pi f t)\right)\\ &\cdot \left(R_0 + R_\mathrm{m}\cos(2\pi f t - \varphi)\right)\end{aligned}$$

$$\begin{aligned}&= \underbrace{\Phi_0 R_0 + \frac{\Phi_\mathrm{m} R_\mathrm{m}}{2}\cos\varphi}_{\text{constant terms}}\\ &\quad + \Phi_0 R_\mathrm{m}\cos(2\pi f t - \varphi) + \Phi_\mathrm{m} R_0 \cos(2\pi f t)\\ &\quad + \underbrace{\frac{\Phi_\mathrm{m} R_\mathrm{m}}{2}\cos\left(2\pi(2f)t - \varphi\right)}_{\text{high frequency terms}}\end{aligned}$$

In fact, the acquired signal is actually the integration of this expression over the time of one frame by the camera. This integration reduces the relative importance of the high frequency terms and we will not discuss them further.

We are left with a signal which contains the thermal information (R_m and φ) but also a second term linked to the constant parts of the reflectivity and LED intensity. This is a usual situation in homodyne detection and we must subtract this term. Taking a second image, this time out of phase,

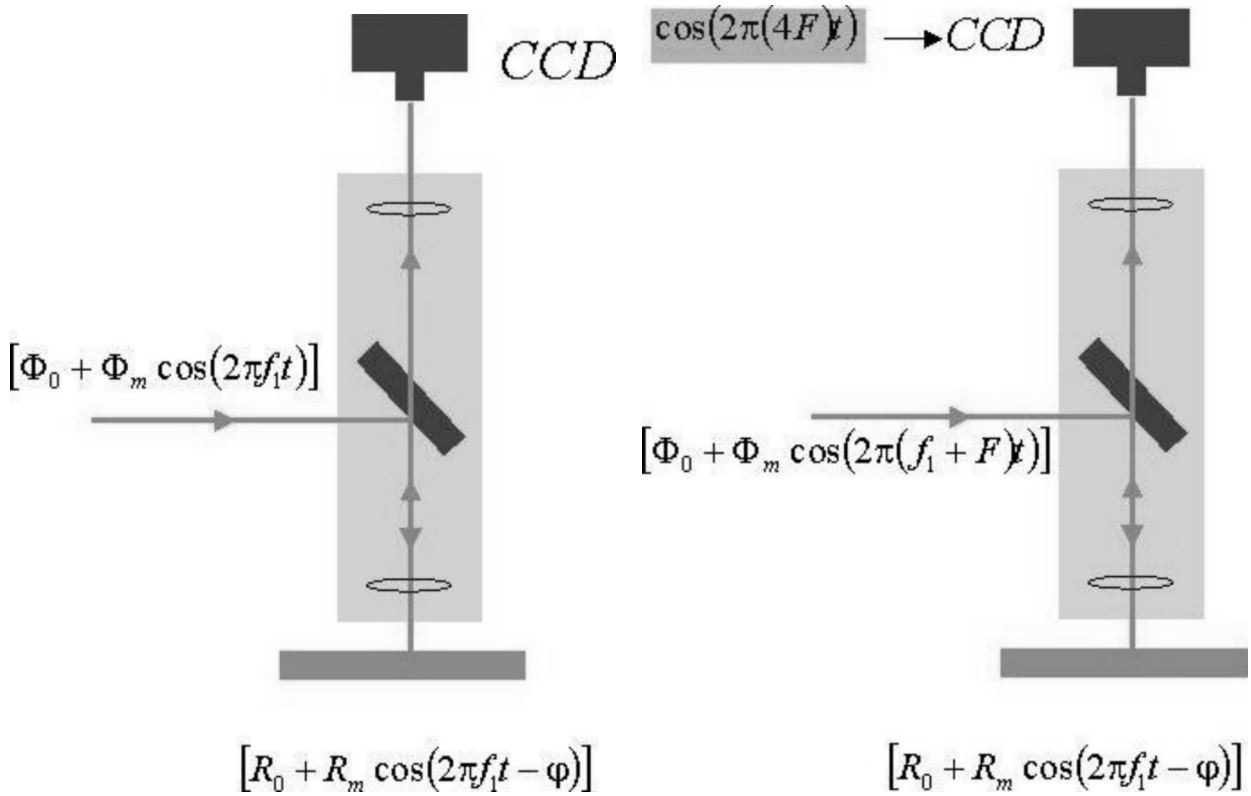

Figure 3. Two stroboscopic setups. In the homodyne setup (left) the LED is modulated at the same frequency as the reflection coefficient (or thermal source). In the heterodyne detection (right) this frequency is slightly shifted.

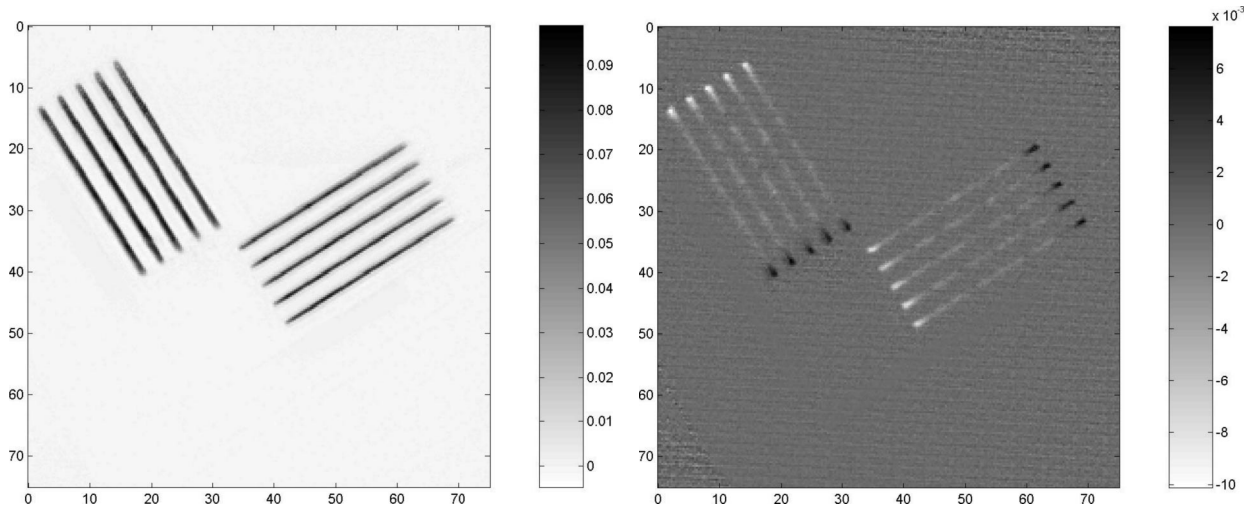

Figure 4. Joule (left) and Peltier (right) heating on 10 polysilicon resistors. The resistances are polysilicon strips. In the case of Joule heating the whole strips are heated. In the case of the Peltier effect, the heating is localized at the intersections with the metal contacts. These images show the real (in phase) part of the photothermal signal.

$$\Phi_0 + \Phi_\mathrm{m}\cos(2\pi f t - \pi) = \Phi_0 - \Phi_\mathrm{m}\cos(2\pi f t)$$

will yield the following constant terms:

$$\Phi_0 R_0 - \frac{\Phi_\mathrm{m} R_\mathrm{m}}{2}\cos\varphi$$

and by subtracting these two images we will obtain the real (or in-phase) component of the photothermal signal: $R_\mathrm{m}\cos\varphi$. Taking two more images (phase shifted by $\pi/2$ and $3\pi/2$) permits us to obtain the imaginary component and, thus, the amplitude and phase of the signal.

Figure 4 is an example of thermal imaging at micron scale of polysilicon resistors associated with metallic bars (nonvisible on the images). We have applied alternative voltage in order to get modulated heat sources. The left image is related to the Joule heating while the right one images the Peltier effect [10]. In the first case, the modulation of frequency of the applied voltage was 25 kHz; Joule heating being a quadratic effect, we expect to see a modulated heat source at the frequency of 50 kHz. We have fixed the modulation frequency of the LED at this value. Peltier heating is a linear effect, when applying voltage at 50 kHz the heating is modulated at the same frequency and again the probe is modulated at 50 kHz.

One of the difficulties in this experiment is the stability of the constant term $\Phi_0 R_0$. We will now consider the heterodyne case, in which this problem is avoided.

2.2. Heterodyne detection

The LED is now modulated at a frequency $f + F$, sligthly shifted from the modulation frequency of the thermoreflectance signal (see *figure 3*, right). The frequency shift, F, will be chosen smaller than half of the camera frame rate. The signal reflected to the camera can now be written as

$$\begin{aligned}\Phi \cdot R &= \big(\Phi_0 + \Phi_\mathrm{m}\cos\big(2\pi(f+F)t\big)\big) \\ &\quad \cdot \big(R_0 + R_\mathrm{m}\cos(2\pi f t - \varphi)\big) \\ &= \underbrace{\Phi_0 R_0}_{\text{const. term}} + \underbrace{\frac{\Phi_\mathrm{m} R_\mathrm{m}}{2}\cos(2\pi F t + \varphi)}_{\text{low frequency term}} \\ &\quad + \Phi_0 R_\mathrm{m}\cos(2\pi f t - \varphi) \\ &\quad + \Phi_\mathrm{m} R_0\cos\big(2\pi(f+F)t\big) \\ &\quad + \underbrace{\frac{\Phi_\mathrm{m} R_\mathrm{m}}{2}\cos\big(2\pi(2f+F)t - \varphi\big)}_{\text{high frequency terms}}\end{aligned}$$

Again we will neglect the high frequency terms. We can see that it is now possible for the camera to sample the low frequency term which contains only the thermal information. We can also envisage implementing a numerical bandpass filter centred on F, to improve the signal-to-noise ratio.

Figure 5 is a photothermal image on the same type of resistors as presented in *figure 4*. The modulation

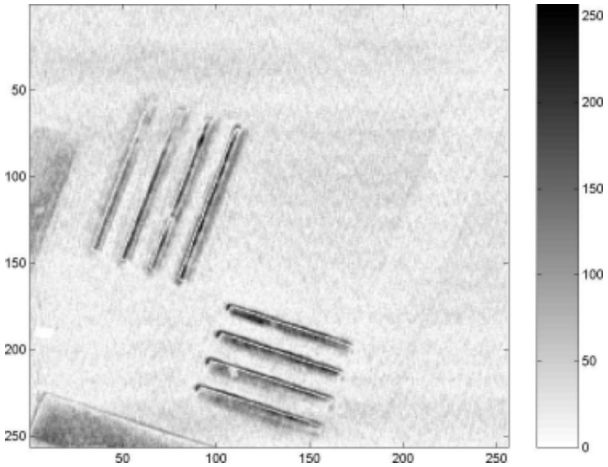

Figure 5. Joule heating on the same type of resistors as shown in *figure 4*, this time using the heterodyne setup. The image shows the amplitude of the signal.

frequency of the current was 20 kHz, thus creating a modulated heat source at 40 kHz. The LED was modulated at 40.01 kHz, producing a "low frequency" photothermal term at 10 Hz. We then set the camera frame rate to 40 Hz to sample this signal.

3. CONCLUSION

With CCD array photothermal microscopy it is now possible to record at micron scale an AC thermal map in a roughly two minutes and without scanning the sample. The stroboscopic approach permits high frequency detection which is a crucial factor in obtaining good spatial resolution. The second setup (heterodyne) will permit us to extend the modulation frequency ranges to the MHz regime while allowing the possibility to include numerical filters in order to improve signal-to-noise ratio.

REFERENCES

[1] Rosencwaig A., Opsal J., Smith W.L., Willenborg D.L., Detection of thermal waves through optical reflectance, Appl. Phys. Lett. 46 (1985) 1013–1015.

[2] Inglehart L.J., Broniatowski A., Fournier D., Boccara A.C., Lepoutre F., Photothermal imaging of copper-decorated grain boundary in silicon, Appl. Phys. Lett. 56 (1990) 1749–1751.

[3] Pottier L., Micrometer scale visualization of thermal waves by photoreflectance microscopy, Appl. Phys. Lett. 64 (1994) 1618–1619.

[4] Pélissonnier C., Pottier L., Fournier D., Thorel A., Local thermal properties of aluminium nitride: a multiscale approach of diffusivity and intergranular structure, in: Meriani S., Sergo V. (Eds.), Fourth Euro Ceramics, Vol. 3, Gruppo Editoriale Faenza Editrice S.p.A., 1995, pp. 413–420.

[5] Pelissonnier-Grosjean C., Jeulin D., Pottier L., Fournier D., Thorel A., Mesoscopic modeling of intergranular structure of Y_2O_3 doped aluminium nitride and application to the prediction of the effective thermal conductivity, Key Engineering Materials 132–136 (1997) 623–626.

[6] Mansanares A.M., Roger J.P., Fournier D., Boccara A.C., Temperature field determination of InGaAsP/InP lasers by photothermal microscopy, evidence for weak nonradiative processes at the facets, Appl. Phys. Lett. 64 (1994) 4–6.

[7] Batista J.A., Mansanares A.M., Da Silva E.C., Fournier D., Photothermal and electroreflectance images of biased metal-oxide semiconductor field effect transistors: six kinds of subsurface microscopy, J. Appl. Phys. 82 (1997) 423–426.

[8] Beaudoin J.-L., Merienne E., Danjoux R., Egee M., Numerical system for infrared scanners and application to subsurface control of materials by photothermal radiometry, SPIE 590, Infrared Technology and Applications (1985) 285–292.

[9] Busse G., Wu D., Karpen W., Thermal wave imaging with phase sensitive modulated thermography, J. Appl. Phys. 71 (1992) 3962–3965.

[10] Forget B.C., Grauby S., Fournier D., Gleyzes P., Boccara A.C., High resolution AC temperature field imaging, Electron. Lett. 33 (1997) 1688–1689.